Physics – Uspekhi **55** (5) 508 – 518 (2012)

INSTRUMENTS AND METHODS OF INVESTIGATION PACS numbers: 42.79.Pw, 79.60.Jv, 85.60.Gz, 88.40.hj

Photoemission from metal nanoparticles

I E Protsenko, A V Uskov

DOI: 10.3367/UFNe.0182.201205e.0543

Contents

Abstract. The approach of A M Brodsky and Yu Ya Gurevich is generalized to photoemission from metal nanoparticles at the excitation of a localized plasmon resonance (LPR) in them. The cross section and the probability amplitude of photoemission from a nanoparticle are obtained analytically, taking into account the LPR excitation and the electromagnetic field and photoelectron mass changes at the metal–environment interface. An increase by two orders of magnitude in the photocurrent from a layer of Au nanoparticles to silicon compared to a bulk Au layer is predicted due to an increase in the electromagnetic field strength under the excitation of LPR and due to a significant part of the nanoparticle surface being nonparallel to the incident field polarization. Practicable applications of the results include improving the performance of photocells and photodetectors, and probably reducing the minimum photoeffect time.

1. Introduction

It is well-known that oscillations of electron density of metal nanoparticles possess a resonance frequency in the visible part of the spectrum or the near-IR spectral range — so-called localized plasmon resonance (LPR). Investigations into the optical and electrophysical effects related to the excitation of LPR and other similar resonances in metal nanoparticles and nanostructures are the concern of a rapidly advancing realm of modern physics — nanoplasmonics. The appearance of LPR is caused by surface charge of the particles [1–4]: the particle boundaries build up a potential well for electron density oscillations of the particle. The LPR frequency of small particles (with characteristic dimensions below 40 nm) depends only slightly on the size of the particles, but more strongly on their shape, the type of metal, and the ambient material.

The LPR may be excited by an external electromagnetic field (EMF). In the case of LPR, the energy is stored both in oscillations of electron density of nanoparticles and in the oscillation-related EMF itself. The EMF energy density at the LPR frequency inside a nanoparticle and within a distance on the order of the LPR wavelength from it turns out to be approximately Q times higher [5] than the energy density of the external EMF that excites the particle (Q is the LPR quality factor which depends on losses, including those for the field scattering by the particle to the environment and absorption in the particle material). Usually in experiments, $Q < 10$ [1–4, 6, 7], although theoretical estimates predict that the value of Q may be as high as several dozen [8].

At the excitation of LPR, a nanoparticle behaves like an EMF cavity. However, unlike, for instance, a Fabry–Perot resonator, also present in the cavity-nanoparticle is the near field, i.e., the charge-related Coulomb field; the near field extends to distances $\leqslant \lambda$ from the particle (λ is the EMF wavelength). The resonance properties of metal nanoparticles (which are frequently referred to as plasmonic [1–4, 8]) and their capacity to 'concentrate' the electromagnetic field inside and around themselves allowed predicting and experimentally observing several new effects [1–4, 8, 9], giant Raman scattering [9] being the most well-known of them. New optoelectronic devices with plasmonic nanoparticles have been proposed and implemented, including sensors [1–4, 9–11], nano-scaled lasers [12–15], and high-efficient solar cells [16–18].

Nanoparticles that are employed in optical devices are sometimes regarded as nanoantennas [1–4, 19, 20]. In the development and modeling of devices which use the optical (plasmonic) properties of metal nanoparticles, it is of interest and value to also investigate the electrophysical properties of

I E Protsenko, A V Uskov Lebedev Physical Institute, Russian Academy of Sciences, Leninskii prosp. 53, 119991 Moscow, Russian Federation; Plasmonics, LLC,
ul. Nizhnie Polya 52/1, 109382 Moscow, Russian Federation
E-mail: protsenk@sci.lebedev.ru, alexusk@sci.lebedev.ru

Received 22 March 2011, revised 10 June 2011
Uspekhi Fizicheskikh Nauk **182** (5) 543 – 554 (2012)
DOI: 10.3367/UFNr.0182.201205e.0543
Translated by E N Ragozin; edited by A Radzig

the contact of plasmonic nanoparticles with their environment, for instance, the contact of the particle with the surface (or the ambient material) whereon (wherein) the nanoparticle is resided. The transfer of charge carriers (electrons or holes) and/or energy from the particle to its environment and back may have a significant influence, either positive or negative, on the properties of a device which comprises nanoparticles, up to complete suppression of LPR and its related effects. For instance, commonly known is the effect of photoluminescence enhancement due to the addition of metal nanoparticles to luminescent objects (for instance, dye molecules in a solution). But when the distance between a luminescent molecule and a nanoparticle is short enough (less than several nanometers), efficient radiationless relaxation occurs, and the luminescence is completely suppressed [1–4, 21].

Photoconverter schemes have been proposed, whereby both the optical plasmonic and electrophysical properties of metal nanoparticles are simultaneously used, for instance, for the electrical connection (commutation) of photoconverter stages [23]. There is evidence that the efficiency of solar photoconverters improves, as stated in Ref. [24], on injecting into a semiconductor substrate the carriers from the electron–hole pairs photoinduced in on-substrate metallic nanoparticles under LPR excitation in the particles. At the same time, the transfer of carriers across the plasmonic nanoparticle–substrate contacts at the excitation of LPR in the particles has been much less studied than their optical properties. This is due to the difficulties encountered in the theoretical and experimental investigations of the electrophysical properties of nano-scaled objects. The study of transport and other electrophysical properties of substrate contacts with metal nanoparticles, performed simultaneously with the investigation into the optical properties of the particles, is required for the development of efficient plasmonic optoelectronic devices [22], including solar photoconverters, photodetectors, nano-scaled light-emitting diodes, and nano-scaled lasers.

Among the effects related to the transfer of carriers under the excitation of nanoparticle LPR is photoemission from nanoparticles, which is theoretically examined in our work. The photoemission from nanoparticles may be substantially different from the photoemission from large (in comparison with the EMF wavelength) macroscopic metallic structures (for instance, from metal layers). This is so because, first, the EMF inside the particle and outside of it, near the nanoparticle surface, rises sharply at LPR excitation and, second, the surface area-to-volume ratio for a nanoparticle is much greater than for macroscopic structures. The latter is of importance, because the main contribution to photoemission is made from the surface photoeffect, when an electron absorbs a photon and escapes from the metal in a collision with the metal surface [25]. Another photoeffect type — a volume photoeffect, whereby a photon is absorbed in the electron collision under the metal surface — makes a smaller contribution [25] and so, as a rule, is neglected in the calculation of photoemission. Third and last, for the surface photoeffect to occur, the intensity of the electric field which excites the electron should have as strong a component as possible perpendicular to the metal surface. Clearly, this condition is easier to fulfill for nanoparticles than for lengthy metal films on which light is incident normally or at a small angle. Therefore, the photoelectron yield per unit metal mass from nanoparticles under LPR excitation would be expected to be higher than from lengthy metal structures like, for instance, metal layers in existing photodetectors [26–28]. Raising the efficiency with the aid of nanoparticles will assist, in particular, in improving the sensitivity of medium- and far-IR photodetectors, which is an important applied problem [29, 30].

To quantitatively estimate the photoemission from nanoparticles and determine the optimal parameters whereby the photoemission is at its maximum, it is necessary to calculate the photoemission cross section for nanoparticles, which is the main objective of our work. The calculation of the surface photoemission cross section for metallic particles with the inclusion of LPR excitation in them, its quantitative estimations, and, proceeding from these estimates, the conclusion that the photoemission from nanoparticles into silicon may be much more efficient than the photoemission from a continuous metal layer constitute one of the main results of our work. We note that the fabrication of micro- and nanostructures on the surface of a photodetector for raising the photoemission efficiency is well known and widely used. In particular, the early 1970s saw the appearance of III – V compound photocathodes (gallium arsenide, etc.).

In numerous publications on these photocathodes (see, for instance, the bibliography in Ref. [31]), it was shown that the photoemission layer has a highly dispersed structure and is not a continuous metallic layer. It is also well-known that all aforementioned photocathodes exhibited a substantially higher photoemission current than the emission from continuous photocathode layers. At the same time, the highly dispersed surface structures of the known photocathodes were not expressly fabricated in such a way that LPR could be excited in the surface particles. In the majority of cases, these structures and the macroscopic metallic coatings are a comprehensive whole, these structures having a good electrical contact with them, and so in the majority of nanoparticles appearing in such structures there is no way of exciting LPR by the incident field and substantially enhancing the photoemission owing to the field 'concentration' factor.

Without fulfilling special conditions for the majority of surface particles, the excitation of LPR may occur only by accident in a small number of 'hot' spots, which may hardly affect the photoemission from the photocathode as a whole. The fact that the photoemission current from the known photocathodes with a highly dispersed surface structure exceeds the emission from continuous layers is attributable primarily to the greater surface area from which the photoemission takes place, to the nonparallelism of the surface and the electric vector of the incident electromagnetic field, and supposedly not to the LPR excitation. The excitation of LPR in the majority of structures of the nanostructured surface will result in an even greater rise in photocurrent, and therefore the investigation of photoemission from nanoparticles on the surface of a photocathode under LPR excitation conditions is a topical and interesting problem.

The utilization of nanoparticle plasmonic properties was proposed for raising the efficiency of photodetectors; however, photoemission from nanoparticles has not been yet considered [32]. The rise in efficiency of the photoemission from metal nanoparticles into a vacuum at the excitation of LPR has been experimentally observed, and its employment was proposed for improving the efficiency of photodetectors [33, 34]. At the same time, a systematic theoretical treatment of the photoemission from nanoparticles and determination

of the photoemission cross section for nanoparticles have not been pursued to date.

The present study is concerned with the treatment, primarily analytical, of the physical aspects of photoemission from metal nanoparticles proceeding from the classical theory set out in detail in monograph [25]. In particular, we calculated the photoemission cross section and found the general expression for the probability amplitude of the photoemission and its cross section. Our calculations suggest that the photoemission current from a gold nanoparticle layer into silicon may be by two orders of magnitude higher than the photocurrent from a continuous gold layer. Furthermore, the theoretical result of Ref. [25] for the photoemission probability was generalized to the case when surface effects are explicitly taken into account: the changes (steps) of electric field strength and electron mass on the particle surface. The inclusion of these surface effects changes (increases in the case under consideration) the photoemission cross section several-fold and is especially important for the photoemission from nanoparticles whose surface area is larger in comparison with that of a continuous metal layer.

The probability and cross section of photoemission derived in our work are the quantities required for the calculation of photocurrent from a layer of metal nanoparticles. The analytical approach adopted in our work is appropriate, because, first, it permits tracing all the details of the physics of the enhancement of photoemission from nanoparticles under LPR excitation. For instance, the rise in photoemission cross section is related not only to the concentration of EMF (which is rather evident), but also to changes in EMF and the mass of a free electron on the surface of a nanoparticle. In this case, quantum-mechanical interference effects of photoelectron dynamics turn out to be significant in the calculation of the cross section. The analytical approach permits us to explicitly separate the contributions which the following three factors make to the photocurrent from the nanoparticle: the photoemission probability, the EMF enhancement in the nanoparticle under LPR excitation, and the nanoparticle surface shape.

In principle, it is possible to 'control' the photoemission by varying these three factors, each separately. For instance, by varying the nanoparticle shape, it is possible to change the peak of the photocurrent spectrum. A detailed discussion of the possibilities of controling the photoemission is beyond the scope of this work. The resultant analytical expressions for the photoemission cross section and probability are more convenient to apply (both in experiment and in the further elaboration of the theory, for instance, in the analysis of the systems of interacting nanoparticles) than numerical results. The analytical approach allowed us to explicitly take into account many features of optical plasmonic effects in nanoparticles, for instance, the dynamic depolarization and radiative loss effects (which would not have been separated in a numerical analysis). Finally, the analytical results may serve as a test model for the numerical analysis of more complex cases, for instance, those which fall outside the scope of the dipole approximation employed in describing the nanoparticle–EMF interaction in our work.

Next, we discuss only the photoemission of electrons into a vacuum or into a uniform dielectric medium surrounding a nanoparticle. However, the approach under consideration may also be applied to the solution of other, more challenging problems related to carrier transfer in the vicinity of nanoparticles. Among these problems are, for instance, the capture of a free carrier by the particle or photoemission from the nanoparticle involving tunneling through a potential barrier [35], including the case where the metallic particle is close to the surface of a semiconductor and is separated from this surface by a thin (tunnel) dielectric layer. The last structure is typical for questions of efficiency improvement in solar elements by using metal nanoparticles [16–18].

The layout of the paper is as follows. In Section 2, we find the general expression for the photoemission probability amplitude with the inclusion of the changes in electromagnetic field strength and the electron mass in the electron passage across the interface between the media, and derive an explicit expression for the photoemission probability amplitude, assuming that the metal boundary is represented by a step-like potential. Section 3 is dedicated to the determination, with the application of the results of Section 2, of the cross section of electron photoemission from the nanoparticle. In Section 4, the results of Section 3 are employed for estimating the cross section of the photoemission from spherical gold nanoparticles into silicon. The resultant data and the lines of future research into photoemission from nanoparticles are discussed in the concluding section.

2. Photoemission probability amplitude with the inclusion of electromagnetic field jump on the media interface and photoemission probability for a boundary in the form of a potential step

2.1 General expression for the photoemission probability amplitude

Using the perturbation theory, Brodsky and Gurevich [25] derived an expression for the photoemission probability amplitude $C_+(\infty)$ for an electron which is traveling through a medium (a metal) along the z-axis perpendicular to the medium boundary, under the action of an electromagnetic field with frequency ω:

$$C_+(\infty) = \frac{|e|m}{\hbar\omega W_1}\int_{-\infty}^{\infty} \mathrm{d}z \left(E_\mathrm{m}\,\frac{\mathrm{d}\Psi_0}{\mathrm{d}z}\,\Psi_{1-} + \frac{1}{2}\,\Psi_{1-}\Psi_0\,\frac{\mathrm{d}E_\mathrm{m}}{\mathrm{d}z}\right). \tag{1}$$

Here, e is the (negative) charge, and m is the electron mass. The medium boundary is described by a one-dimensional potential (barrier) $V(z)$ (Fig. 1). The effective electron mass changes on exit from the metal, and therefore $m = m(z)$. In expression (1) and further, Ψ_0, $\Psi_{1\pm}$ are the electron wave functions in states with a total energy E_i, $i = 0$, 1 below and above the potential barrier, $E_\mathrm{m} \equiv E/m(z)$, E is the amplitude of the electric field component directed along the z-axis, and

$$W_1(\Psi_{1-}\Psi_{1+}) = \Psi_{1-}\,\frac{\mathrm{d}\Psi_{1+}}{\mathrm{d}z} - \Psi_{1+}\,\frac{\mathrm{d}\Psi_{1-}}{\mathrm{d}z}\,.$$

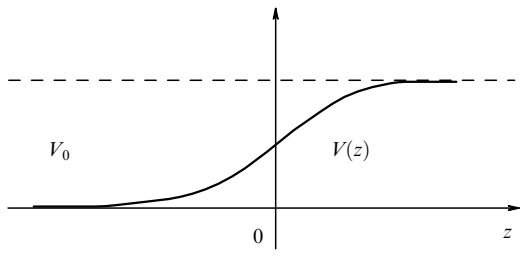

Figure 1. Potential barrier for a moving electron.

The resultant expression for the photoemission probability was derived in Ref. [25] under the assumption that the electric field E is constant along the z-axis. However, this is not so at the intersection of the media interface because, due to the surface charge, a change in the normal field component[1] occurs on the surface, i.e., one must consider function $E(z)$. We invoke the approach of Ref. [25] in the case of $E(z)$ and $m = m(z)$, and rearrange expression (1) into the form

$$C_+(\infty) = \frac{|e|m}{W_1(\hbar\omega)^2}\int_{-\infty}^{\infty}\frac{\mathrm{d}z}{m}(c_V + c_E + c_m)\,, \tag{2}$$

where c_V, c_E, and c_m describe the photoemission with the inclusion of the steps, respectively, of the potential, the electromagnetic field, and the effective electron mass at the media interface:

$$\begin{aligned} c_V &= -EV'\Psi_0\Psi_{1-}\,,\\ c_E &= E'\left[\frac{\hbar^2}{2m}\,\Psi_0'\Psi_{1-}' + \left(E_0 - V + \frac{\hbar\omega}{2}\right)\Psi_0\Psi_{1-}\right], \\ c_m &= -\frac{Em'}{m}\left(E_0 - V + \frac{\hbar\omega}{2}\right)\Psi_0\Psi_{1-}\,. \end{aligned} \tag{3}$$

A detailed derivation of expressions (2) from formula (1) will be published in Ref. [36]. Below, we integrate expression (2) for the case of piecewise linear (step) functions $V(z)$, $E(z)$, and $m(z)$, which have a discontinuity at $z = 0$ and are constant for $z \neq 0$. For them, one obtains $V' = V\delta(z)$, $E' = (E_+ - E_-)\delta(z)$, and $m' = (m_0 - m)\delta(z)$, where $E_\pm$ are the respective values of E on the right and left of $z = 0$, and m and m_0 are the effective electron masses in the metal and outside it, respectively. The values at the interface are as follows: $V(0) = V/2$, $E(0) = (E_+ + E_-)/2$, and $m(0) = (m_0 + m)/2$. And finally, a prime in functions Ψ_0', Ψ_{1-}' entering Eqn (3) and below stands for differentiation over z.

2.2 Wave functions in the absence of perturbation

Let us find the wave functions of an electron which travels perpendicular to the metal boundary described by a one-dimensional potential barrier in the form of a step (Fig. 2). An electron with a charge e and an effective mass m for $z < 0$ and $m = m_0$ for $z > 0$ travels in the step potential

$$V(z) = \begin{cases} 0\,, & z < 0\,,\\ V/2\,, & z = 0\,,\\ V\,, & z > 0\,. \end{cases} \tag{4}$$

The electron Hamiltonian is $H = H_-$ for $z < 0$, and $H = H_+$ for $z > 0$:

$$H_- = -\frac{\hbar^2}{2m}\frac{\mathrm{d}^2}{\mathrm{d}z^2}\,, \qquad H_+ = -\frac{\hbar^2}{2m_0}\frac{\mathrm{d}^2}{\mathrm{d}z^2} + V\,. \tag{5}$$

By solving the Schrödinger equation $\mathrm{i}\hbar(\partial\bar{\Psi}_{0+}/\partial t) = H_+\bar{\Psi}_{0+}$, we find the wave function $\bar{\Psi}_{0+} = \Psi_0\exp[-\mathrm{i}(E_0/\hbar)t]$ of the state with the total energy $E_0 < V$ for an electron which is incident on the barrier from the left and is reflected from it:

$$\Psi_0 = \left[\exp(\mathrm{i}k_0 z) + A_0\exp(-\mathrm{i}k_0 z)\right]_{z<0} + \left[B_0\exp(\mathrm{i}\tilde{k}_0 z)\right]_{z>0}\,, \tag{6}$$

[1] The metal boundary in Fig. 1 is a smooth function of z, and so the variation of the electric field at the interface is also a smooth function of z.

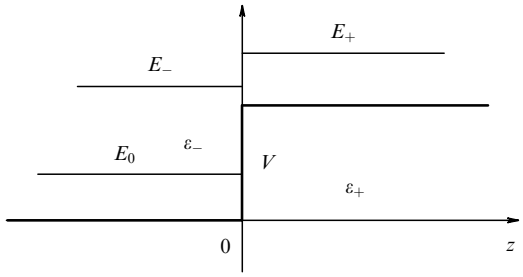

Figure 2. Potential barrier in the form of a step. Shown are the discontinuity of the electric field at $z = 0$ — at the point of discontinuity of the potential — and permittivities of the metal (ε_-) and the particle environment (ε_+).

where the wave numbers are given by

$$k_0 = \frac{1}{\hbar}(2mE_0)^{1/2}\,, \qquad \tilde{k}_0 = \frac{1}{\hbar}\left[2m_0(E_0 - V)\right]^{1/2}. \tag{7}$$

Since $V > E_0$, the quantity $(E_0 - V)^{1/2} = \mathrm{i}(V - E_0)^{1/2}$ is purely imaginary. For convenience, the wave function Ψ_0 is normalized in such a way that the coefficient of the term $\exp(\mathrm{i}k_0 z)$, which describes the initial electron state — the incidence on the barrier from $z = -\infty$ — is taken equal to 1.

The coefficients A_0 and B_0 in expression (6) are determined from the continuity conditions at $z = 0$:

$$\begin{aligned} &\Psi_0(z = -0) = \Psi_0(z = +0)\,,\\ &m^{-1}\left(\frac{\partial\Psi_0}{\partial z}\right)_{z=-0} = m_0^{-1}\left(\frac{\partial\Psi_0}{\partial z}\right)_{z=+0}\,, \end{aligned} \tag{8}$$

which are equivalent to the equations $1 + A_0 = B_0$ and $1 - A_0 = \theta_0 B_0$, whence it follows that

$$A_0 = \frac{1 - \theta_0}{1 + \theta_0}\,, \quad B_0 = \frac{2}{1 + \theta_0}\,, \quad \theta_0 = \left[\frac{m}{m_0}\left(1 - \frac{V}{E_0}\right)\right]^{1/2}. \tag{9}$$

In a similar way, we find the wave functions $\bar{\Psi}_{1\pm} = \Psi_{1\pm}\exp[-\mathrm{i}(E_1/\hbar)t]$ for the electron state with a total energy $E_1 > V$, where

$$\Psi_{1+} = \left[A_{1+}\exp(\mathrm{i}k_1 z) + B_{1+}\exp(-\mathrm{i}k_1 z)\right]_{z<0} + \exp(\mathrm{i}\tilde{k}_1 z)_{z>0}\,, \tag{10}$$

$$\Psi_{1-} = \left[A_{1-}\exp(\mathrm{i}\tilde{k}_1 z) + B_{1-}\exp(-\mathrm{i}\tilde{k}_1 z)\right]_{z>0} + \exp(-\mathrm{i}k_1 z)_{z<0}\,, \tag{11}$$

and the real wave numbers are defined as

$$k_1 = \frac{1}{\hbar}(2mE_1)^{1/2}\,, \qquad \tilde{k}_1 = \frac{1}{\hbar}\left[2m_0(E_1 - V)\right]^{1/2}. \tag{12}$$

The coefficients $A_{1\pm}$ and $B_{1\pm}$ are determined from the wave-function continuity conditions at $z = 0$, similar to conditions (8), which lead to the equations $A_{1\pm} + B_{1\pm} = 1$, $A_{1+} - B_{1+} = \theta_1$, and $\theta_1(B_{1-} - A_{1-}) = 1$, where

$$\theta_1 = \left[\frac{m}{m_0}\left(1 - \frac{V}{E_1}\right)\right]^{1/2};$$

whence it follows that

$$\begin{aligned} A_{1+} &= \frac{1 + \theta_1}{2}\,, \qquad B_{1+} = \frac{1 - \theta_1}{2}\,,\\ A_{1-} &= \frac{\theta_1 - 1}{2\theta_1}\,, \qquad B_{1-} = \frac{1 + \theta_1}{2\theta_1}\,. \end{aligned} \tag{13}$$

Wave function (10) and (11) make up the fundamental system of solutions to the Schrödinger equation with the electron Hamiltonian (5).

2.3 Expression for the photoemission probability amplitude

Following the procedure proposed in Ref. [25], we treat the action of the monochromatic EMF of frequency ω on an electron as the perturbation

$$\hat{U}_{\text{pert}}\left(z, \frac{\mathrm{d}}{\mathrm{d}z}\right)\cos(\omega t) = \frac{1}{2}\,\hat{U}_{\text{pert}}\left(z, \frac{\mathrm{d}}{\mathrm{d}z}\right)\left(\exp(-\mathrm{i}\omega t) + \exp(\mathrm{i}\omega t)\right),$$

in Hamiltonian (5). The action of operator $\hat{U}_{\text{pert}}$ on the electron-state wave function Ψ_i ($i = 0, 1\pm$) is defined by the expression

$$\hat{U}_{\text{pert}}\Psi_i = \frac{\mathrm{i}\hbar e}{2c}\left[\frac{\mathrm{d}}{\mathrm{d}z}\left(\frac{A}{m}\,\Psi_i\right) + \frac{A}{m}\,\frac{\mathrm{d}\Psi_i}{\mathrm{d}z}\right] + e\varphi\Psi_i\,,$$

where e is the electron charge, c is the speed of light in vacuum, A is the z-component of the vector potential of the EMF in the medium, and φ is the scalar potential of the EMF.

Calculations with wave functions (10) and (11) lead to the expression (its detailed derivation will be published in Ref. [36])

$$\left.\frac{W_1}{m}\right|_{z<0} = \left.\frac{W_1}{m_0}\right|_{z>0} = \mathrm{i}\,\frac{k_1}{m}(1+\theta_1) \equiv \mathrm{i}\left(\frac{k_1}{m} + \frac{\tilde{k}_1}{m_0}\right). \tag{14}$$

At $z = 0$, considering that Ψ_0' and Ψ_{1-}' are discontinuous functions, so that $\Psi_{0,1-}'(0) = (1/2)[\Psi_{0,1-}'(-0) + \Psi_{0,1-}'(+0)]$, we find

$$\Psi_0\Psi_{1-} = \frac{2}{1+\theta_0}\,, \qquad \Psi_0'\Psi_{1-}' = \frac{2\tilde{k}_0 k_1 \bar{m}^2}{m_0 m(1+\theta_0)}\,. \tag{15}$$

Hereinafter, the following notations are introduced $\bar{m} = (m_0 + m)/2$, $\Delta m = m_0 - m$, $\bar{E} = (E_+ + E_-)/2$, and $\Delta E = E_+ - E_-$. We substitute expressions (14) and (15) into expression (2) to obtain, on rearrangement, an explicit expression for the photoemission probability amplitude

$$C_+(\infty) = \frac{2|e|m}{\mathrm{i}k_1\bar{m}(\hbar\omega)^2(1+\theta_0)(1+\theta_1)} \times\left\{-V\bar{E} + \frac{\Delta E}{2}\left[E_1^{1/2} + (E_0 - V)^{1/2}\right]^2 - \frac{\bar{E}\Delta m}{2\bar{m}}(E_0 + E_1 - V)\right\}. \tag{16}$$

We express formula (16) in terms of the variable $x = (\hbar k_0)^2/(2mV) \equiv E_0/V$. Taking into consideration that

$$k_1 = \frac{\sqrt{2mV}}{\hbar}\left(x + \frac{\hbar\omega}{V}\right)^{1/2}, \qquad \theta_0 = \left[\frac{m}{m_0}\left(\frac{1}{x} - 1\right)\right]^{1/2},$$
$$\theta_1 = \left\{\frac{m}{m_0}\left[1 - \left(x + \frac{\hbar\omega}{V}\right)^{-1}\right]\right\}^{1/2},$$

we arrive at the resultant expression for the photoemission probability:

$$\left|C_+(\infty)\right|^2 = C_0 U(x)\left|K_{\text{dis}}(x)\right|^2, \tag{17}$$

where the dimensionless coefficient is

$$C_0 = \frac{2|e|^2|E_-|^2 V}{m\hbar^2\omega^4}\,, \tag{18}$$

$$U(x) = \frac{4r_{\text{m}}^2}{(r_{\text{m}}+1)^2} \times\frac{x}{\left[x + r_{\text{m}}(1-x)\right]\left\{(x+\hbar\omega/V)^{1/2} + \left[r_{\text{m}}(x+\hbar\omega/V-1)\right]^{1/2}\right\}^2}\,, \tag{19}$$

$$r_{\text{m}} = \frac{m}{m_0}\,,$$

$$K_{\text{dis}}(x) = \frac{1}{2}\left(1 + \frac{\varepsilon_-}{\varepsilon_+}\right)\left[1 + \frac{1 - r_{\text{m}}}{1 + r_{\text{m}}}\left(2x + \frac{\hbar\omega}{V} - 1\right)\right] + \frac{1}{2}\left(1 - \frac{\varepsilon_-}{\varepsilon_+}\right)\left[\left(x + \frac{\hbar\omega}{V}\right)^{1/2} + \mathrm{i}(1-x)^{1/2}\right]^2. \tag{20}$$

The factor K_{dis} describes the influence of the discontinuities in the electromagnetic field and the effective electron mass at the metal boundary where $z = 0$, and expression (19) for $U(x)$ also turns out to depend on the step in the effective electron mass. To revert to the case considered in Ref. [25], where the steps in electron mass and electromagnetic field amplitude at the metal boundary were neglected, one must put $r_{\text{m}} = 1$ and $\varepsilon_- = \varepsilon_+$ in formulas (19) and (20), resulting in $K_{\text{dis}}(x) = 1$ and $U(x) = x/[(x+\hbar\omega/V)^{1/2} + (x+\hbar\omega/V-1)^{1/2}]^2$.

Therefore, the electron photoemission probability, when the boundary has the form of a potential step and the steps in effective electron mass and electromagnetic field amplitude at the media interface are taken into account, is defined by expression (17), where the coefficient C_0 is given by formula (18), and expressions for $U(x)$ and $K_{\text{dis}}(x)$ are defined by formulas (19) and (20), respectively. These formulas will be employed below in calculating the cross section of photoemission from nanoparticles.

3. Cross section for photoemission from a nanoparticle for a stepwise potential

3.1 Expression for the photoemission cross section

By definition, the cross section σ_{pe} of photoemission from a nanoparticle is given by

$$\sigma_{\text{pe}} = \frac{J_{\text{pe}}}{I}\,, \tag{21}$$

where J_{pe} is the total photocurrent from the nanoparticle (in electrons per second), and I is the intensity of an external monochromatic field which causes the photoemission at the point where the particle is located (in photons cm^{-2} s^{-1}). The photocurrent from the particle is

$$J_{\text{pe}} = \int_{\text{surf}} j\,\mathrm{d}s = \int_{\text{surf}} j(\theta,\varphi,r) r\,\mathrm{d}r\,\sin\theta\,\mathrm{d}\theta\,\mathrm{d}\varphi\,, \tag{22}$$

where j is the density of photocurrent (in electrons cm^{-2} s^{-1}) normal to the particle surface at the surface point defined by the polar angle θ, the azimuthal angle φ, and the distance r from the origin to the particle surface (Fig. 3).

Following Refs [14, 21], we go over from the one-dimensional model of electron motion to the three-dimensional one. Then, according to formula (2.30) from Ref. [25],

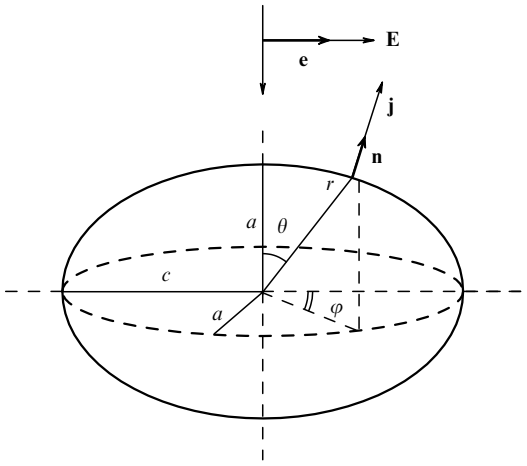

Figure 3. Photocurrent density j at the surface point defined by the angles θ and φ for a spheroidal nanoparticle excited by an external electromagnetic field of amplitude E. The lengths of two particles' semiaxes are the same and equal to a; the length of the third semiaxis is c.

the photocurrent density $\mathrm{d}j$ for those electrons which had energy in the interval from E_0 to $E_0 + \mathrm{d}E_0$ in the domain of the particle (i.e., below the barrier), absorbed photons and overcame the barrier is expressed as

$$\mathrm{d}j = \frac{\hbar\tilde{k}_{1z}}{m}\,|C_+|^2\Theta\left[k_{0z}^2 + \frac{2m}{\hbar^2}(\hbar\omega - V)\right]\mathrm{d}n_0\,, \tag{23}$$

where $\hbar\tilde{k}_{1z}/m$ is the velocity of such electrons above the potential barrier, $\mathrm{d}n_0 \equiv 2f_\mathrm{F}(k_0)\,\mathrm{d}k_{0x}\,\mathrm{d}k_{0y}\,\mathrm{d}k_{0z}/(2\pi)^3$ is the number of these electrons, and

$$f_\mathrm{F}(k_0) = \left(1 + \exp\frac{(\hbar k_0)^2/(2m) - \varepsilon_\mathrm{F}}{k_\mathrm{B}T}\right)^{-1}$$

is the Fermi distribution function. Moreover, k_0 is the magnitude of the electron wave vector prior to photon absorption, $k_0^2 = k_{0x}^2 + k_{0y}^2 + k_{0z}^2$, $k_{0x,y}$ are the electron wave vector components parallel to the particle surface, ε_F is the Fermi energy of the metal which makes up the particle, k_B is the Boltzmann constant, and T is the temperature. Since $2mE_0/\hbar^2 = k_0^2$, one has for the step barrier:

$$\begin{aligned}\tilde{k}_{1z} &= \sqrt{\frac{2m}{\hbar^2}(E_0 + \hbar\omega - V) - (k_{0x}^2 + k_{0y}^2)} \\ &\equiv \sqrt{k_{0z}^2 + \frac{2m}{\hbar^2}(\hbar\omega - V)}\,.\end{aligned} \tag{24}$$

The last formula stands for the z-component of the electron wave vector behind the barrier (denoted as $\tilde{k}_1$ in the one-dimensional case; see formula (12)), k_{0z} is the wave vector component of the electron inside the nanoparticle, which is perpendicular to its surface, $|C_+|^2 \equiv |C_+(\infty)|^2$ is the photoemission probability, and Θ is the theta function. The photocurrent density j of arbitrary-energy electrons is written out as

$$\begin{aligned}j = \frac{2}{(2\pi)^3}\int \mathrm{d}k_{0x}\,\mathrm{d}k_{0y}\,\mathrm{d}k_{0z}\,f_\mathrm{F}(\mathbf{k}_0)\,\frac{\hbar\tilde{k}_{1z}}{m}\,|C_+|^2 \\ \times\,\Theta\left[k_{0z}^2 + \frac{2m}{\hbar^2}(\hbar\omega - V)\right].\end{aligned} \tag{25}$$

In the last expression, only f_F depends on $k_{0x,y}$, and so it is possible to take the integral with respect to $\mathrm{d}k_{0x}\,\mathrm{d}k_{0y}$ using the substitutions $k_{0x}^2 + k_{0y}^2 = c^2$ and $\int_0^\infty \mathrm{d}x\,(1 + e^x/b)^{-1} = \ln(1+b)$:

$$\begin{aligned}&\int \mathrm{d}k_{0x}\,\mathrm{d}k_{0y}\,f_\mathrm{F}(\mathbf{k}_0) \\ &\quad= \pi\int_0^\infty \frac{\mathrm{d}c^2}{1 + \exp\left\{\left[\hbar^2(c^2 + k_{0z}^2)/(2m) - \varepsilon_\mathrm{F}\right]/k_\mathrm{B}T\right\}} \\ &\quad= \frac{2\pi m k_\mathrm{B}T}{\hbar^2}\ln\left[1 + \exp\frac{\varepsilon_\mathrm{F} - \hbar^2k_{0z}^2/(2m)}{k_\mathrm{B}T}\right].\end{aligned} \tag{26}$$

Substituting expressions (23), (24), and (26) into formula (25) and considering that $|C_+|^2 \sim |E_-|^2$, then according to expressions (17), (18) one obtains the photoemission current density at some point on the nanoparticle's surface:

$$\begin{aligned}&j = C_\mathrm{em}|E_-|^2\,, \\ &C_\mathrm{em} = \frac{|e|^2k_\mathrm{B}TV^2}{\pi^2\hbar^5\omega^4}\int_{0;\,1-\hbar\omega/V}^1 \mathrm{d}x\left(1 + \frac{\hbar\omega/V - 1}{x}\right)^{1/2} \\ &\qquad\times\ln\left(1 + \exp\frac{\varepsilon_\mathrm{F} - Vx}{k_\mathrm{B}T}\right)U(x)\left|K_\mathrm{dis}(x)\right|^2,\end{aligned} \tag{27}$$

where the lower integration limit is equal to 0 if $\hbar\omega > V$, and equal to $1 - \hbar\omega/V$ if $\hbar\omega < V$; we took into account that $E_0 < V$ and, consequently, $x < 1$; $U(x)$ and $K_\mathrm{dis}(x)$ are defined by expressions (19) and (20), respectively.

If we neglect the thermal excitation of electrons above the Fermi surface, i.e., move to the limit $T \to 0$ in expression (27), and make use of the condition $\exp[(\varepsilon_\mathrm{F} - Vx)/(k_\mathrm{B}T)] \to \infty$, we may then write, instead of formula (27), the following relationship

$$\begin{aligned}C_\mathrm{em} = \frac{|e|^2}{\pi^2}\,\frac{V^3}{\hbar^5\omega^4}\int_{0;\,1-\hbar\omega/V}^{\varepsilon_\mathrm{F}/V} \mathrm{d}x\left(1 + \frac{\hbar\omega/V - 1}{x}\right)^{1/2} \\ \times\left(\frac{\varepsilon_\mathrm{F}}{V} - x\right)U(x)\left|K_\mathrm{dis}(x)\right|^2;\end{aligned} \tag{28}$$

in this case, it is required that $\hbar\omega > V - \varepsilon_\mathrm{F}$ and the lower integration limit be equal to 0 if $\hbar\omega > V$. Therefore, one finds

$$J_\mathrm{pe} = C_\mathrm{em}\int_\mathrm{surf}|E_-|^2\,\mathrm{d}s\,. \tag{29}$$

Here, the integral is taken over the particle's surface, and C_em is independent of the coordinates of the surface point; the normal field component $E_- = (\mathbf{E}_\mathrm{int}\mathbf{n})$, where $\mathbf{E}_\mathrm{int}$ is the electric field inside the particle, and $\mathbf{n}$ is the vector of the surface normal to the particle's surface at a given surface point. The field components tangent to the particle's surface have no influence on the photoemission probability. The electron motion along the particle's surface under the action of tangential field components affects, in principle, the electron distribution function; however, in relatively low fields typical for photoemission cases, this effect is negligible, much weaker than ordinary particle heating in the course of electromagnetic field absorption.

The electric field inside the particle is related to the external field $\mathbf{E}$ incident on the particle by the relation $\mathbf{E}_\mathrm{int} = \hat{F}(\mathbf{r})\mathbf{E}$, where $\hat{F}(\mathbf{r})$ is a tensor. For the spheroidal particles to be considered below, the field inside the particle

is uniform, and thus $\hat{F}$ is a constant quantity independent of $\mathbf{r}$. For simplicity, we assume that vector $\mathbf{E}$ is parallel to one of the major axes of the spheroidal particle; then, $\mathbf{E}_{\rm int} = F\mathbf{E}$, where F is a quantity independent of $\mathbf{r}$. For nonspherical particles, F depends on which of the major particle's axes is parallel to $\mathbf{E}$. Therefore, one has

$$J_{\rm pe} = C_{\rm em}|F|^2 K_{\rm geom}|E|^2 , \tag{30}$$

where $K_{\rm geom} = \int_{\rm surf}(\mathbf{ne})$, and $\mathbf{e}$ is the unit vector in the direction of external field polarization (see Fig. 3). In view of formula (21), and taking into consideration that the external field intensity I (in photons cm^{-2} s^{-1}) is of the form

$$I = \frac{1}{8\pi}\,\frac{cn_+|E|^2}{\hbar\omega} ,$$

we arrive at the photoemission cross section

$$\sigma_{\rm pe} = \frac{8\pi\hbar\omega}{cn_+}\,C_{\rm em}|F|^2 K_{\rm geom} , \tag{31}$$

where c is the speed of light in vacuum, and $n_+ = {\rm Re}\,\sqrt{\varepsilon_+}$ is the refractive index of the medium outside the nanoparticle.

3.2 Parameters F and $K_{\rm geom}$

According to Ref. [40], the field parameter F for spheroidal particles is given by

$$F = \frac{1}{1 + R_{\rm dep} - {\rm i}R_{\rm rad}}\,\frac{\varepsilon_+}{\varepsilon_+ + (\varepsilon_- - \varepsilon_+)L} , \tag{32}$$

where the second multiplier is the result of calculations in the framework of the quasistatic approximation [38], and the factor

$$L = \frac{r^2}{2}\int_0^\infty \frac{{\rm d}u}{(u + r^2)^2(u + 1)^{1/2}} ,$$

where the aspect ratio $r = a/c$, a is the length of one of the two equal semiaxes of the ellipsoidal particle, and c is the length of the third semiaxis (see Fig. 3). The first multiplier in formula (32) takes into account the effects of dynamic depolarization and radiative loss with the aid of the factors $R_{\rm dep}$ and $R_{\rm rad}$, respectively [39]:

$$\begin{aligned} R_{\rm dep} &= \frac{\varepsilon_- - \varepsilon_+}{\varepsilon_+ + (\varepsilon_- - \varepsilon_+)L}(A\varepsilon_+ y^2 + B\varepsilon_+^2 y^4) , \\ R_{\rm rad} &= \frac{16\pi^3}{9}\,\frac{n_+^3}{r}\left(\frac{a}{\lambda}\right)^3 \frac{\varepsilon_- - \varepsilon_+}{\varepsilon_+ + (\varepsilon_- - \varepsilon_+)L} , \\ A &= -0.4865L - 1.046L^2 + 0.848L^3 , \\ B &= 0.01909L + 0.1999L^2 + 0.6077L^3 , \end{aligned} \tag{33}$$

where $y = \pi a/\lambda$, and λ is the wavelength of the electromagnetic field in vacuum. The factor $R_{\rm dep}$ characterizes the departure of the electromagnetic field inside the nanoparticle from the uniform one. Electron collisions with the particle's surface have the result that the dielectric constant ε_- of the particle's metal is different from the dielectric constant $\varepsilon_{\rm bulk}$ of a macroscopic specimen of this same metal. This difference may be taken into account in the following way [3]:

$$\varepsilon_- = \varepsilon_{\rm bulk} + \frac{\omega_{\rm pl}^2}{\omega^2 + {\rm i}\omega\gamma_0} - \frac{\omega_{\rm pl}^2}{\omega^2 + {\rm i}\omega(\gamma_0 + {\rm i}Av_{\rm F}/a)} , \tag{34}$$

where $\omega_{\rm pl}$ and γ_0 are the plasma frequency and the radiation loss-induced damping increment, respectively, $v_{\rm F}$ is the electron velocity at the Fermi surface, and A is a constant on the order of unity, which depends on the particle shape. According to Ref. [40], the shape parameter $K_{\rm geom}$ takes the form

$$K_{\rm geom} = \frac{\pi a^2}{r}\left[\frac{r}{1 - r^2} + \frac{1 - 2r^2}{(1 - r^2)^{3/2}}\,\arcsin(1 - r^2)^{1/2}\right] . \tag{35}$$

Thus, the photoemission cross section is defined by expression (31), where the $C_{\rm em}$ factor is expressed by formula (27), while the factors F and $K_{\rm geom}$ are defined by formulas (32) and (35), respectively. The photoemission cross section may be compared with the cross sections for absorption ($\sigma_{\rm abs}$) and scattering ($\sigma_{\rm sc}$) of light by a particle [40]:

$$\begin{aligned} &\sigma_{\rm abs} = \frac{8\pi^2 a^3 n_+}{3r\lambda}\,{\rm Im}\,\alpha , \qquad \sigma_{\rm sc} = \frac{128\pi^5 a^6 n_+^4}{27r^2}\,|\alpha|^2 , \\ &\alpha = \frac{1}{1 + R_{\rm dep} - {\rm i}R_{\rm rad}}\,\frac{\varepsilon_- - \varepsilon_+}{\varepsilon_+ + (\varepsilon_- - \varepsilon_+)L} . \end{aligned} \tag{36}$$

Proceeding from these results, we will make in the next section numerical estimates of the photoemission cross sections for metal nanoparticles.

4. Photoemission from gold nanoparticles into silicon

By way of example, we calculate the photoemission cross section for a spherical gold nanoparticle embedded in p-type silicon. The latter was selected as the nanoparticle's environment, because the work function $\chi_{\rm e}$ in the transfer of an electron from gold to p-type silicon is low: $\chi_{\rm e} = 0.34$ eV [41]. Since the Fermi energy for gold $\varepsilon_{\rm F} = 5.1$ eV [41], the potential barrier height $V = \varepsilon_{\rm F} + \chi_{\rm e} = 5.44$ eV. The respective conduction electron masses in gold and silicon are $m = 0.992m_{\rm e} \approx m_{\rm e}$ and $m_0 = 0.25m_{\rm e}$ [42], where $m_{\rm e}$ is the free electron mass in a vacuum. Therefore, $r_{\rm m} = 0.992/0.25 = 3.968$. The data on gold dielectric constant $\varepsilon_{\rm Au}$ were borrowed from Ref. [43]. Dielectric constant (34) of the metal nanoparticle (gold) is conveniently written as a function of EMF wavelength λ in a vacuum:

$$\varepsilon_-(\lambda) = \varepsilon_{\rm Au}(\lambda) + \left(\frac{\lambda}{\lambda_{\rm p}}\right)^2\left[\frac{1}{1 + {\rm i}\lambda/\lambda_{\rm c}} - \frac{1}{1 + ({\rm i}\lambda/\lambda_{\rm c})(a_{\rm c}/a + 1)}\right] . \tag{37}$$

The following parameter values were taken in the calculation: $\lambda_{\rm p} = 0.142$ μm, $\lambda_{\rm c} = 55$ μm, which correspond to the best approximation

$$\varepsilon_{\rm Au}(\lambda) \approx 12 + \left(\frac{\lambda}{\lambda_{\rm p}}\right)^2 \frac{1}{1 + {\rm i}\lambda/\lambda_{\rm c}} \tag{38}$$

in the range of wavelengths λ of interest from 0.6 to 1.2 μm, which contains the LPR of the spherical gold particle put in silicon under consideration; $a_{\rm c} = Av_{\rm F}\lambda_{\rm c}/(2\pi c_0)$ is a parameter which characterizes electron collisions with the particle's surface, $A = 0.7$, and $v_{\rm F} = (2E_{\rm F}|e|/m_0)^{1/2} \approx 1.3 \times 10^6$ m s^{-1}. The conduction electron mass in gold is assumed to be practically equal to the free electron mass.

Shown in Fig. 4 for $a = 10$ nm are the real and imaginary parts of $\varepsilon_{\rm Au}(\lambda)$, its approximations according to formula (38)

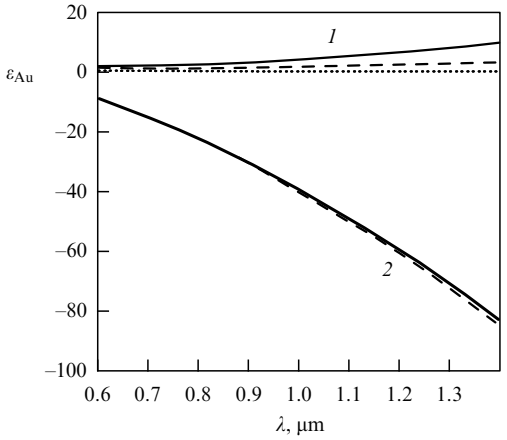

Figure 4. Imaginary (*1*) and real (*2*) parts of the dielectric constant of gold [the dashed line is drawn according to Ref. [43], and the solid one according to formula (37)]. The dotted horizontal line corresponds to zero.

(they are rather close), and $\varepsilon_-(\lambda)$ obtained by formula (37). One can see that the imaginary part of $\varepsilon_-(\lambda)$ significantly exceeds $\mathrm{Im}\,[\varepsilon_{Au}(\lambda)]$, which points out the importance of including electron collisions with the nanoparticle's surface in the estimation of its dielectric constant. For the dielectric constant $\varepsilon_+(\lambda)$ of silicon, which accommodates the gold nanoparticle, we take advantage of the analytical approximation derived in Ref. [44]:

$$\varepsilon_+(\lambda) = \varepsilon_\infty + \sum_{i=1}^{3} C_i \left[1 - \left(\frac{1.242}{\lambda E_i}\right)^2 - \mathrm{i}\,\frac{1.242}{\lambda E_i}\,\gamma_i\right]^{-1} - F_1\chi_1^{-2}(\lambda)\ln\left[1-\chi_1^2(\lambda)\right] - F_2\chi_2^{-2}(\lambda)\ln\frac{1-\chi_1^2(\lambda)}{1-\chi_2^2(\lambda)},$$

where

$$\chi_i(\lambda) = \left(\frac{1.242}{\lambda} + \mathrm{i}\Gamma_i\right)\frac{1}{E_i}$$

and $\varepsilon_\infty = 0.2$, $C_1 = 0.77$, $C_2 = 2.96$, $C_3 = 0.3$, $F_1 = 5.22$, $F_2 = 4$, $\gamma_1 = 0.05$, $\gamma_2 = 0.1$, $\gamma_3 = 0.1$, $E_1 = 3.38$, $E_2 = 4.27$, $E_3 = 5.3$, $\Gamma_1 = 0.08$, and $\Gamma_2 = 0.1$.

Figure 5a displays the absorption and scattering cross sections (in πa^2 units) calculated by formulas (36) for a gold nanoparticle in silicon. One can see that the absorption cross section exceeds πa^2 by more than an order of magnitude in the vicinity of $\lambda = \lambda_{LPR} = 0.857$ μm. Figure 5b depicts the factor $|F|^2$, which enters into formula (31) and accounts for the increase in field intensity in the nanoparticle, in comparison with the field intensity outside the particle; F is defined by expression (32). At the LPR frequency, the electric field intensity inside the particle is more than 150 times higher than the outside field intensity.

The cross section σ_{pe} of the photoemission from a spherical gold nanoparticle of radius $a = 10$ nm in silicon, which was obtained using formula (31) with the aid of expressions (27), (32), and (35), is plotted in Fig. 6a as a function of incident radiation wavelength; also plotted here are the absorption (σ_{abs}) and scattering (σ_{sc}) cross sections.

As is clear from Fig. 6a, the photoemission cross section at the LPR peak amounts to about a half of the geometrical cross section πa^2, which is equal to 4.2% of the maximum

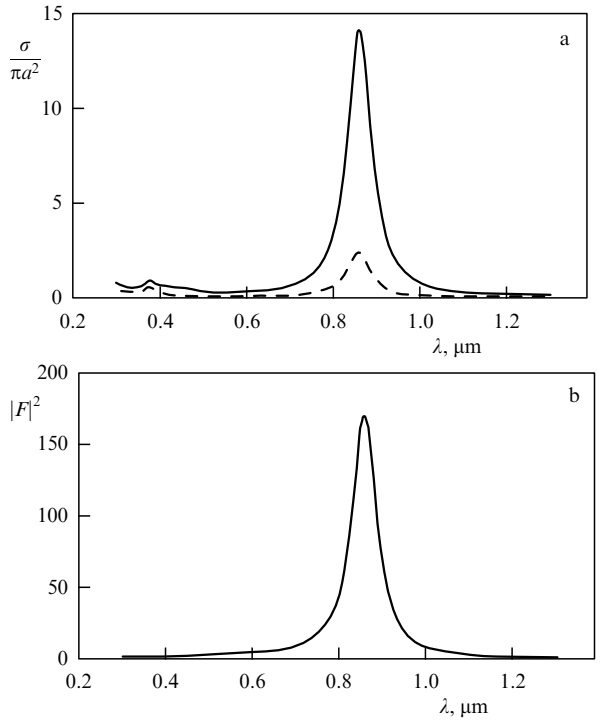

Figure 5. (a) Absorption σ_{abs} (solid line) and scattering σ_{sc} (dashed line) cross sections for a spherical gold nanoparticle in silicon. (b) Factor of field intensity enhancement in the nanoparticle.

value of σ_{abs}. The ratio σ_{pe}/σ_{abs} at the resonance, i.e., for $\lambda = \lambda_{LPR}$, is plotted in Fig. 6b and characterizes the relative fraction of the energy absorbed by the nanoparticles that is transferred to photoemission current. Although this fraction is small, several percent, it turns out to be appreciably larger than for a continuous gold layer (see this section below). Figure 6b demonstrates that the σ_{pe}/σ_{abs} ratio decreases almost linearly from 9 to 1% as the nanoparticle's radius lengthens from 1 to 20 nm. Therefore, the photoemission efficiency is higher for small particles. At the same time, the absorption cross section itself is small for short particle radii a (due to LPR broadening arising from electron collisions with the surface of the particle). As the nanoparticle's radius increases, the magnitude of σ_{abs} reaches its maximum and then becomes smaller due to dephasing and radiative loss (Fig. 6c). Therefore, the optimal particle's radius may rather be estimated proceeding from the magnitude of photoemission current (see this section below).

In the calculation of the photoemission current induced by an ensemble of nanoparticles, collective effects can play a significant role, including particle–particle interactions via the EMF. A comprehensive description of collective effects is a difficult task, which lies outside the scope of the present paper. And so we will restrict ourselves to simple and rather crude estimates of collective effects, reserving for the future a detailed analysis of their influence on photoemission.

Proceeding from the fact that the number of photons absorbed in a layer of nanoparticles per unit time may not exceed the number of photons incident on the layer from the outside per unit time, one can deduce that $\sigma_{abs}/(\pi a^2) < 1/\eta$, where η is the relative surface nanoparticle density (the fraction of surface area occupied by the nanoparticles), i.e., σ_{abs} becomes smaller with an increase in η. The decrease in σ_{abs} with an increase in η is practically due to the LPR broadening caused by collective effects, which is evidenced

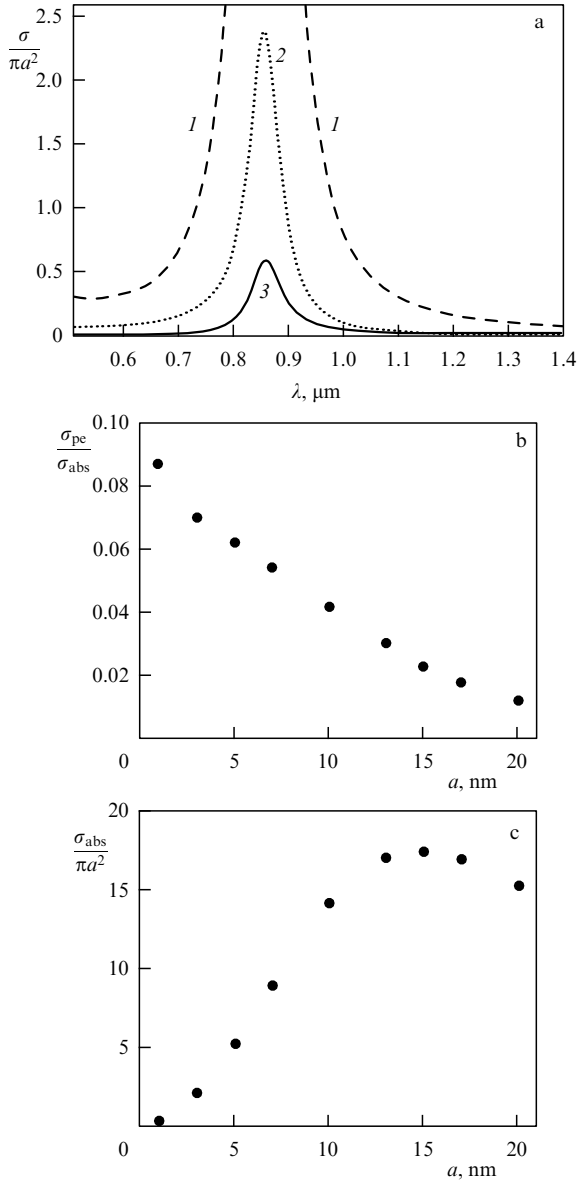

Figure 6. (a) Photoemission cross section of a gold nanoparticle (curve *3*) and its absorption (curve *1*) and scattering (curve *2*) cross sections in units of πa^2, i.e. the geometrical cross section of the nanoparticle. (b) Ratio σ_{pe}/σ_{abs} at the LPR maximum for different radii of spherical gold nanoparticles. (c) Absorption cross section of a spherical gold nanoparticle as a function of its radius.

in experiments. The LPR broadening caused by collective effects supposedly decreases also the factor F, as well as the photoemission cross section for a narrow EMF spectrum, i.e., when $\lambda = \lambda_{LPR}$, but this does not signify that the photoemission from an ensemble of nanoparticles for a broad spectrum (for instance, solar) will necessarily weaken with increasing η. Furthermore, narrow lines of high-Q LPRs were predicted and observed in nanoparticle ensembles in special cases [45]. This signifies that the effective factor F may turn out to be quite high in nanoparticle ensembles, even if σ_{abs} is not large.[2] Hence, one cannot *a priori* draw a conclusion that collective effects undoubtedly lower the efficiency of photoemission from nanoparticles.

As noted above, a detailed investigation of the influence of collective effects on the photoemission from nanoparticles is rather complicated and goes beyond the scope of this study. Therefore, we compare the photoemission from nanoparticles with the photoemission from a thin continuous layer of gold in silicon by taking advantage of the foregoing formulas derived neglecting collective effects.

We estimate the photoemission current density j_{pe}^0 for a thin continuous layer of gold using formula (27), where E_- is the EMF component normal to the metal surface. For simplicity we assume that the EMF is incident on the metal surface at a grazing angle, i.e., $E_- = E$ (the EMF amplitude). Since the grazing incidence (whereby the angle of EMF incidence on the metal surface is equal to 90°) is hard to realize, we will knowingly overestimate the density of photoemission current from the continuous gold layer.

Let us assume now that there is a layer of spherical gold nanoparticles with a relative surface density η in silicon and estimate the surface density of photoemission current from this layer under solar irradiation. The solar radiation spectrum normalized to unity may be written out as

$$w_s(\lambda) = \frac{\lambda^{-4}/0.128}{\exp(2.616/\lambda) - 1},$$

where λ is the wavelength in micrometers. The surface density j_{pe} of photoemission current from the layer of nanoparticles reduced to the total intensity I of solar radiation is expressed as

$$\frac{j_{pe}}{I} = \frac{\eta}{\pi a^2} \int w_s(\lambda)\sigma_{pe}(\lambda)\,d\lambda\,. \qquad (39)$$

Figure 7a shows the ratio between the surface density of photoemission current from the layer of spherical gold nanoparticles and the surface density of photoemission current from the continuous gold layer at $\eta = 0.3$ (i.e., 30% of the surface area is covered with nanoparticles) as a function of the nanoparticle radius for the spectral range from 0.32 to 2 μm, which takes in approximately 80% of solar radiation energy.

Figure 7b exhibits the same for the monochromatic EMF at the wavelength of localized plasmonic resonance. As is evident from Fig. 7a, the solar radiation-induced photoemission current from the nanoparticle layer is several times higher than the photoemission current induced by the continuous gold layer; in this case, there exists an optimal nanoparticle radius which maximizes the photoemission current. Without the inclusion of collective effects, the photoemission current from the nanoparticles at the frequency of plasmonic resonance and their photoemission cross section are several hundred times higher than the corresponding quantities for the continuous gold layer (Fig. 7b). In the case under consideration, the optimal particle radius is equal to 10 nm. Of course, the resultant data apply to internal photoemission: the problem of the extraction efficiency of photoinduced carriers to an external circuit is not considered. As discussed above, the estimates made above are rather course. Apart from collective effects, they disregard, for instance, the fact that a nanoparticle and its environment (silicon) are separated by a potential barrier and do not form a potential well. Carrier tunneling is possible

[2] It is well known that local fields in ensembles of nanoparticles sufficiently high for a surface photoeffect may emerge not only inside the nanoparticles, but also outside them, in the regions between closely located particles in the proximity to their surfaces [Ref. 4, p. 257].

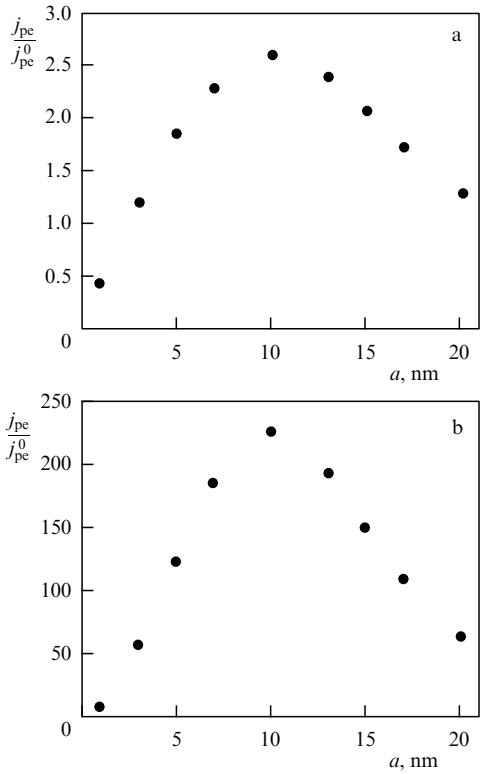

Figure 7. (a) Ratio between the surface density of photoemission current from a layer of spherical gold nanoparticles (with a surface density of 30%) and the surface density of photoemission current from a thin continuous gold layer in silicon as a function of the particle radius a. (b) The same at a wavelength λ_{LPR}.

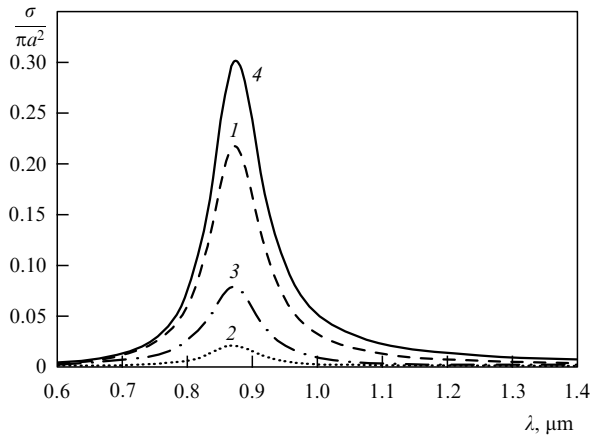

Figure 8. Photoemission cross sections on neglecting the step in the effective electron mass (curve *1*), in the EMF (curve *2*), in the effective mass and the EMF (curve *3*) — the result in accordance with Ref. [25]; with the inclusion of all steps (curve *4*).

in the case of a barrier [35]; furthermore, the probability of transition through the barrier in the photoemission may be higher than the probability of photoemission from a potential well. The potential barrier can be included instead of the potential well using the method of the present study, resulting in an increase in the photoemission cross section. An additional positive, though small, contribution to the photoemission current will be made by volume photoemission, which was not considered in our study and may be treated following, for instance, Fowler's classical work [37].

In this paper, unlike Ref. [25], the resultant expression for the photoemission cross section takes into account the step in normal component of the electric field and the step in the effective mass of conduction electrons at the nanoparticle–environment interface. Let us estimate the significance of these factors in the calculation of the cross section for the photoemission from a gold nanoparticle into silicon. What one has to do to revert to the results of Ref. [25] is to follow the advice given in the paragraph after formula (20). Figure 8 shows the photoemission cross sections with neglect of only the step in the effective mass, i.e., when $r_m = 1$, or of only the EMF step, i.e., when $\varepsilon_-/\varepsilon_+ = 1$, or of both steps, i.e., when $r_m = \varepsilon_-/\varepsilon_+ = 1$. Also plotted in Fig. 8 is the photoemission cross section obtained for $r_m \neq 1$ and $\varepsilon_-/\varepsilon_+ \neq 1$ — the same as curve *3* in Fig. 6.

According to Fig. 8, the inclusion of EMF discontinuity and of the step in the effective electron mass significantly (several-fold) changes the photoemission cross section in the example under consideration. Interestingly, the highest value of the cross section results when all discontinuities are taken into account, i.e., the field and mass jumps enhance the photoemission in this event. The results given in Fig. 8 suggest that in the general case both discontinuities — of the electron mass and the EMF — are significant and should be included in the theory. However, in special cases, for instance when $\varepsilon_-/\varepsilon_+$ is close to unity or photoemission takes place from gold into a vacuum, so that r_m is close to unity, the discontinuity of the corresponding quantity turns out insignificant.

Interestingly, the step in electron mass in the absence of a field jump results in a lowering of the photoemission cross section (comparing with the result of Ref. [25], where the steps were disregarded, cf. curves *2* and *3* in Fig. 8). The field jump in the absence of the mass step increases σ_{pe} (compare curves *1* and *3* in Fig. 8), but a simultaneous accounting of all the steps leads to a maximum increase in σ_{pe} (compare curve *4* with the other curves in Fig. 8). This 'nonadditive' influence of EMF and electron mass jumps on the photoemission cross section is a consequence of the quantum-mechanical nature of the photoemission.

Indeed, although the terms c_V, c_E, and c_m, which describe respectively the photoemission with the inclusion of the steps in the potential, the electromagnetic field, and the effective electron mass at the media interface, enter additively into expression (2) for the photoemission probability amplitude $C_+(\infty)$, the quantity $C_{em} \sim |C_+(\infty)|^2$ enters into expression (31) for σ_{pe}. It turns out that a significant quantum-mechanical interference of the contributions from the terms c_V, c_E, and c_m may occur in the calculation of σ_{pe}. This may result, as is evident from the example, in increasing σ_{pe} when both steps are taken into account, and in an increase or a decrease in σ_{pe} when account is taken of only the EMF jump or of only the step in the effective electron mass.

5. Conclusions

In this study we derived the expression for the probability amplitude and calculated the cross section for the photoemission from metal nanoparticles. By the example of a spherical gold nanoparticle embedded in p-type silicon, the photoemission cross section at a wavelength $\lambda = \lambda_{LPR}$, which corresponds to the excitation of localized plasmonic resonance in the nanoparticle, was shown to amount to several percent of its absorption cross section (which far exceeds the geometrical

cross section of the nanoparticle at resonance); the photoemission cross section is equal to about a half of the geometrical cross section of the nanoparticle (Fig. 6a). Therefore, when the relative surface nanoparticle layer density is $\eta = 0.3$, at $\lambda = \lambda_{\mathrm{LPR}}$ approximately 0.5η, i.e., 15%, of all photons will be converted into photoelectrons — the internal photoemission efficiency at the LPR frequency.

The photoemission current from a layer of nanoparticles at $\lambda = \lambda_{\mathrm{LPR}}$ may be two orders of magnitude higher than the photoemission current from a continuous gold layer. Under irradiation by a broad solar spectrum, the nanoparticles yield a photoemission current several-fold higher than that from a continuous metal layer (see Fig. 7). There is an optimal radius of metal nanoparticles, which maximizes the photoemission current (see Fig. 7). The increase in photoemission from the nanoparticles in comparison with a continuous metal layer is due both to an increase in electric field intensity inside the nanoparticles under LPR excitation (see Fig. 5) and to the fact that a substantial part of the nanoparticle's surface is normal to the direction of polarization of the electromagnetic field incident on the nanoparticles.

The theory of Ref. [25] for the photoemission from metals was generalized: in the calculation of the photoemission cross section we took into account the discontinuities in the effective mass of conduction electrons and the normal component of the electric field strength at the metal–environment interface. The corresponding analytical expressions were obtained; using the example of photoemission from gold nanoparticles in silicon, it was shown that the inclusion of these discontinuities significantly (several-fold) changes the magnitude of the cross section.

In the calculations we neglected the volume photoeffect which increases the photocurrent, and the potential curve at the nanoparticle–environment interface was approximated by a rectangular potential well. The inclusion of a potential barrier, which is possible to tunnel through, would increase the photoemission current. Computations involving more complex potential wells can be performed by way of direct generalization of the method described in this paper. In the future, in passing from separate nanoparticles to their ensembles, when investigating photoemission there is good reason to include collective effects in the interaction of nanoparticles via the EMF. These effects will have an impact only on the factor F, which describes the field inside the particles. Using our approach, it is possible to analyze the capture of carriers by metal nanoparticles.

The results of our work may be utilized in the development of new high-sensitivity photodetectors and photoconverters of light to electric energy. For photodetectors, for instance, of the utmost importance is the question of the shortest attainable photoeffect time and of ways to experimentally determine this time [31]. It is not unlikely that an improvement in photoemission efficiency under the excitation of LPR in nanoparticles will permit shortening the minimal time required to obtain the photoeffect. For instance, if a femtosecond laser pulse attainable with modern lasers is capable of exciting the LPR in a nanoparticle (the answer to this question is the subject of a separate theoretical work), a photodetector with such nanoparticles will be able to afford a femtosecond temporal resolution, even though the nanoparticle material photoresponse time may be longer than the laser pulse duration.

References

1. Maier S A *Plasmonics*: *Fundamentals and Applications* (New York: Springer, 2007)
2. Novotny L, Hecht B *Principles of Nano-optics* (Cambridge: Cambridge Univ. Press, 2006)
3. Brongersma M L, Kik P G (Eds) *Surface Plasmon Nanophotonics* (Kik: Springer, 2007)
4. Klimov V V *Nanoplazmonika* (Nanoplasmonics) (Moscow: Fizmatlit, 2009)
5. Wang F, Shen Y R *Phys. Rev. Lett.* **97** 206806 (2006)
6. Hövel H et al. *Phys. Rev. B* **48** 18178 (1993)
7. Schuller J A et al. *Nature Mater.* **9** 193 (2010)
8. Khlebtsov N G *Kvantovaya Elektron.* **38** 504 (2008) [*Quantum Electron.* **38** 504 (2008)]
9. Kneipp K, Moskovits M, Kneipp H (Eds) *Surface-enhanced Raman Scattering*: *Physics and Applications* (Berlin: Springer-Verlag, 2006)
10. Homola J, Yee S S, Gauglitz G *Sensors Actuators B* **54** 3 (1999)
11. Zhao J et al. *Nanomedicine* **1** (2) 219 (2006)
12. Bergman D J, Stockman M I *Phys. Rev. Lett.* **90** 027402 (2003)
13. Protsenko I E et al. *Phys. Rev. A* **71** 063812 (2005)
14. Noginov M A et al. *Nature* **460** 1110 (2009)
15. Oulton R F et al. *Nature* **461** 629 (2009)
16. Catchpole K R, Polman A *Opt. Express* **16** 21793 (2008)
17. Atwater H A, Polman A *Nature Mater.* **9** 205 (2010)
18. Dement'eva O V et al., in *Vtoroi Mezhdunarodnyi Forum po Nanotekhnologiyam* (*Rusnanotech-2009*) (The Second Nanotechnology International Forum), *Moscow, 6–9 October 2009*
19. Mühlschlegel P et al. *Science* **308** 1607 (2005)
20. Greffet J-J *Science* **308** 1561 (2005)
21. Klimov V V *Usp. Fiz. Nauk* **173** 1008 (2003) [*Phys. Usp.* **46** 979 (2003)]
22. Monestier F et al. *Solar Energy Mater. Solar Cells* **91** 405 (2006)
23. Rand È P, Forrest S R, Patent US2006032529(A1) (2006)
24. Westphalen M et al. *Solar Energy Mater. Solar Cells* **61** 97 (2000)
25. Brodsky A M, Gurevich Yu Ya *Teoriya Elektronnoi Emissii iz Metallov* (Theory of Electron Emission from Metals) (Moscow: Nauka, 1973)
26. Sze S M *Physics of Semiconductor Devices* (New York: Wiley, 1981) [Translated into Russian (Moscow: Mir, 1984)]
27. Soole J B D, Schumacher H *IEEE J. Quantum Electron.* **27** 737 (1991)
28. Ito M, Wada O *IEEE J. Quantum Electron.* **QE-22** 1073 (1986)
29. Piotrowski J, Galus W, Grudzien M *Infrared Phys.* **31** 1 (1991)
30. Yu Z et al. *Appl. Phys. Lett.* **89** 151116 (2006)
31. Shchelev M Ya *Usp. Fiz. Nauk* **170** 1002 (2000) [*Phys. Usp.* **43** 931 (2000)]; Schelev M Ya *Usp. Fiz. Nauk* **182** 649 (2012) [*Phys. Usp.* **55** 611 (2012)]
32. Hetterich J et al. *IEEE J. Quantum Electron.* **43** 855 (2007)
33. Nollé É, Shchelev M Ya *Pis'ma Zh. Tekh. Fiz.* **30** (8) 1 (2004) [*Tech. Phys. Lett.* **30** 304 (2004)]
34. Nolle E, Shchelev M Ya *Zh. Tekh. Fiz.* **75** (11) 136 (2005) [*Tech. Phys.* **50** 1528 (2005)]
35. Nolle É L *Usp. Fiz. Nauk* **177** 1133 (2007) [*Phys. Usp.* **50** 1079 (2007)]
36. "Dipole nano-lasers and related devices" *Electromagnetic Radiation*, InTech, to be published
37. Fowler R H *Phys. Rev.* **38** 45 (1931)
38. Uskov A V et al., in *Sbornik Tezisov Dokladov Uchastnikov Vtorogo Mezhdunarod. Foruma po Nanotekhnologiyam* (Abstracts of the Second Nanotechnology International Forum) (Moscow, 2009) p. 94
39. Bottcher C J F *Theory of Electric Polarization* Vol. 1 (Amsterdam: Elsevier, 1952)
40. Meier M, Wokaun A *Opt. Lett.* **8** 581 (1983)
41. Dutta A, Mazhari B, Visweswaran G S *Semiconductor Devices, Schottky Barrier Height* (Dehli: NPTEL Online-IIT, 2011); http://nptel.iitm.ac.in/courses/Webcourse-contents/IIT-Delhi/Semiconduc... 2009
42. Kittel Ch *Introduction to Solid State Physics* (New York: Wiley, 1956) [Translated into Russian (Moscow: Fizmatgiz, 1962)]
43. Weber M J *Handbook of Optical Materials* (Boca Raton: CRC Press, 2003)
44. Adachi S, Mori H, Ozaki S *Phys. Rev. B* **66** 153201 (2002)
45. Hicks E M et al. *Nano Lett.* **5** 1065 (2005)